11 December 1998

ELSEVIER

Chemical Physics Letters 298 (1998) 129–140

CHEMICAL PHYSICS LETTERS

Femtosecond dynamics of valence-bond isomers of azines: transition states and conical intersections

Dongping Zhong, Eric W.-G. Diau, Thorsten M. Bernhardt, Steven De Feyter, John D. Roberts, Ahmed H. Zewail *

Arthur Amos Noyes Laboratory of Chemical Physics, California Institute of Technology, Pasadena, CA 91125, USA

Received 18 September 1998; in final form 5 October 1998

Abstract

In this Letter, we report the ultrafast dynamics of isomerization and ring opening of azines, using femtosecond-resolved mass spectrometry. The experimental results and theoretical DFT/ab initio calculations elucidate the reaction mechanism and indicate the crucial role of conical intersections in driving these forbidden, ground-state processes. The global motion, initiated by fs wavepackets, is an important concept for nonradiative and reactive processes in polyatomics. © 1998 Elsevier Science B.V. All rights reserved.

1. Introduction

Many chemical reactions having overall small energy changes are regarded as 'forbidden' and have large energy barriers above the ground state. In the description of such reactions by the Woodward–Hoffmann rules, they exhibit unfavorable orbital symmetry correlations. The ground state of the reactants correlates with the excited state of the products, and vice versa. The barriers in such cases are, therefore, made by the 'crossing' of two potential energy surfaces (PESs) and the transition states are defined accordingly.

The crossing or near-crossing of PESs is a well-known problem in polyatomic molecules since the early work by E. Teller, G. Herzberg and others, and has become the subject of theoretical studies for many decades. In particular, the relevance of conical intersections (CIs) to nonradiative relaxations and to photochemical and thermal reactions has been the focus of many articles and books (see, e.g., Refs. [1–4], and references therein). In all of these studies, one must consider the breakdown of the Born–Oppenheimer approximation as the nuclei make their nonadiabatic journey between reactants and products.

A classic problem, where CIs play a major role, is that of reactions involving the isomers of benzene and azines. Over a century, several valence structures for the ground state of benzene have been proposed: Kekulé, Dewar, Hückel (benzvalene type), Ladenburg (prismane type) and Thiele (see Ref. [5]). The well-established aromatic structures are represented by the electron-delocalized or resonance expression of the Kekulé formula, and isomers, such as the Dewar structures, have much higher energies. Thus, ground-state thermal reactions involve a high energy barrier to reach any of the isomers. But, in addition, the conversion of benzene to Dewar ben-

* Corresponding author. E-mail: zewail@cco.caltech.edu

0009-2614/98/$ - see front matter
PII: S0009-2614(98)01160-9

zene is formally considered as a disrotatory 4π-ring closure reaction, forbidden on the ground state. However, from the excited state it is possible to populate these isomers directly.

Experimentally, the exploration of the reaction dynamics is possible provided: (a) a wavepacket is prepared in the reactant valley, prior to reaching the CI; and (b) sufficient energy is supplied to cross over the forbidden region. Both requirements can be satisfied by femtosecond-resolved mass spectrometry as developed in this laboratory for studies of complex reactions [6].

In this Letter, we report studies of pyridine and its possible high-energy isomers, such as one of the two Dewar structures:

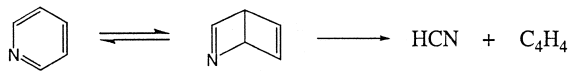

The energy change in this isomerization for one thing involves dearomatization, the loss of ~ 40 kcal/mol of resonance energy. Then, the net change of making of σ and π bonds and breaking of two π bonds is expected to be -20 kcal/mol. Account

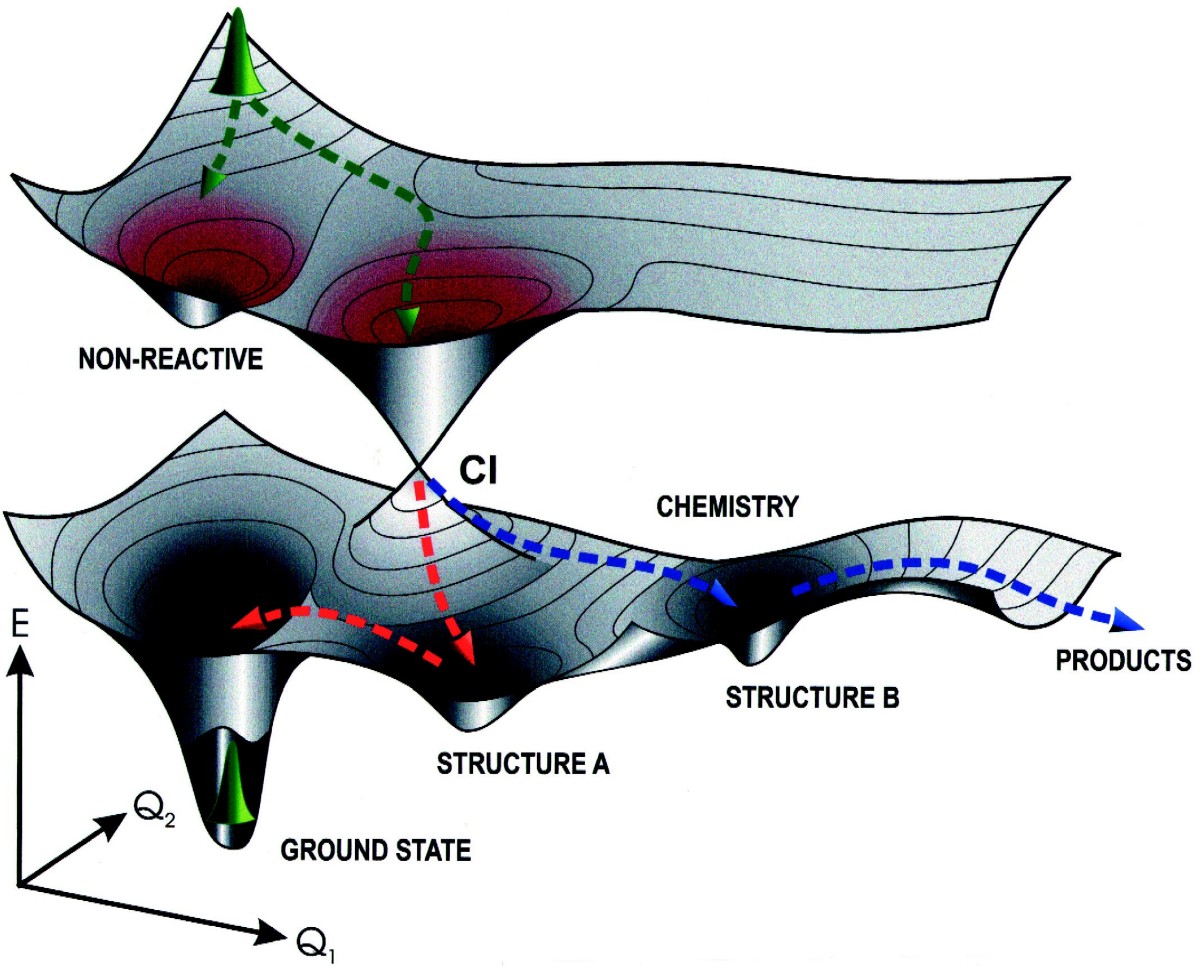

Fig. 1. Schematic representation of the two potential energy surfaces, illustrating ground-state reactions reached through conical intersections. The wavepacket and its reactive and non-reactive trajectories are displayed. No recurrences on the upper surface are shown for simplicity.

must also be taken of strain energy of ~50 kcal/mol. Thus, as will be shown below, the overall energy of the pertinent Dewar structure would be ~70 kcal/mol above that of aromatic pyridine. The ring-opening reaction of pyridine involves the C–N bond breakage (~70 kcal/mol); in contrast, C–C bond breakage requires ~85 kcal/mol.

By using femtosecond (fs) pulses, together with the mass spectra, we are able to observe the wavepacket motion and examine the molecular changes involved in the isomerization. The crucial role of CIs (Fig. 1) and their influence on the nonradiative processes are elucidated. In order to compare the experimental and theoretical results of structures and rates, we have carried out DFT/ab initio calculations at G2M level. For comparison, we also studied other azines, namely, pyrimidine, triazine, and substituted (deuterium and methyl) pyridines. All these studies were made at total energies of 99–103 kcal/mol. At a higher energy (186 kcal/mol), we were able to study the ring-opening process.

2. Experimental

All experiments were performed in a two-chamber molecular beam apparatus integrated with fs laser systems and a time-of-flight (TOF) mass spectrometer. For experiments at 277 nm (and 282 and 288 nm) excitation, a synchronously pumped dye laser was used. For the study of two-photon excitation of pyridine at 307 nm, we employed a colliding pulse mode-locked ring dye laser (CPM). The details of both fs laser systems have been described [6]. Typically the pulse width from the CPM is 90 fs and from the other system is 300 fs. As shown elsewhere [7], the direction of polarization can be altered, relative to the TOF axis, to obtain information about the anisotropy and kinetic energy release. All experiments were done for the monomer beam condition [7], and all samples were purchased from Aldrich (purity ~99%). Care was taken in the analysis of all transients by scanning each for three different time scales. For example, for pyridine, three scans were made: short (~12 ps); intermediate (~40 ps) and long (~100 ps). This way we were able to determine accurately and with consistency the time constants and the amplitude of each component.

3. Theoretical calculations

Calculations of the PES for the isomerization reaction path were performed at G2M(RCC6) level of theory [8]. First, the geometries of the pyridine molecule, isomers, transition states and products were optimized at the B3LYP/6-311G(d, p) level. Then, vibrational frequencies of all species were calculated at the same level of theory in order to characterize the nature of the stationary points, determine the zero-point energy correction for the PES, and calculate the statistical (RRKM) microcanonical reaction rates. Second, a series of high-level ab initio calculations was carried out at the MP4/6-311G(d, p), CCSD(T)/6-31G(d, p) and MP2/6-311 + G(3df, 2p) levels of theory. An additive scheme was implemented to determine more reliable energies using the modified Gaussian-2 (G2M) method to approximate the CCSD(T)/6-311 + G(3df, 2p) calculation.

The DFT/ab initio results are shown in Fig. 2 and Scheme 1. Because of the presence of nitrogen, the Hückel, Dewar and Ladenburg structures have three, two and one isomers, respectively. Two Dewar (D_1 and D_2) isomers lie at energies of 69 and 78 kcal/mol, respectively, above the aromatic Kekulé structure (0 energy). The three Hückel (H_1, H_2 and H_3) isomers have energies of 62, 67 and 82 kcal/mol, respectively. The H_1 isomer has the lowest energy among all isomers and the Ladenburg isomer has the highest energy, 112 kcal/mol. On the isomerization pathway, the D_1 structure has the lowest isomerization barrier of 90 kcal/mol and the D_2 isomer has a higher barrier of 106 kcal/mol. The H_1, H_2 and H_3 isomers have barriers of 92, 94 and 101 kcal/mol, respectively. For the Ladenburg isomer, the barrier is the highest, 152 kcal/mol. On the decomposition side of the isomers, the D_1 structure has the lowest barrier, 111 kcal/mol, to form HCN and 1,3-cyclobutadiene, and all others have barriers of >115 kcal/mol. From our calculations, we can identify the structure of the transition state as having a 'diradical' character for isomerization to the Hückel

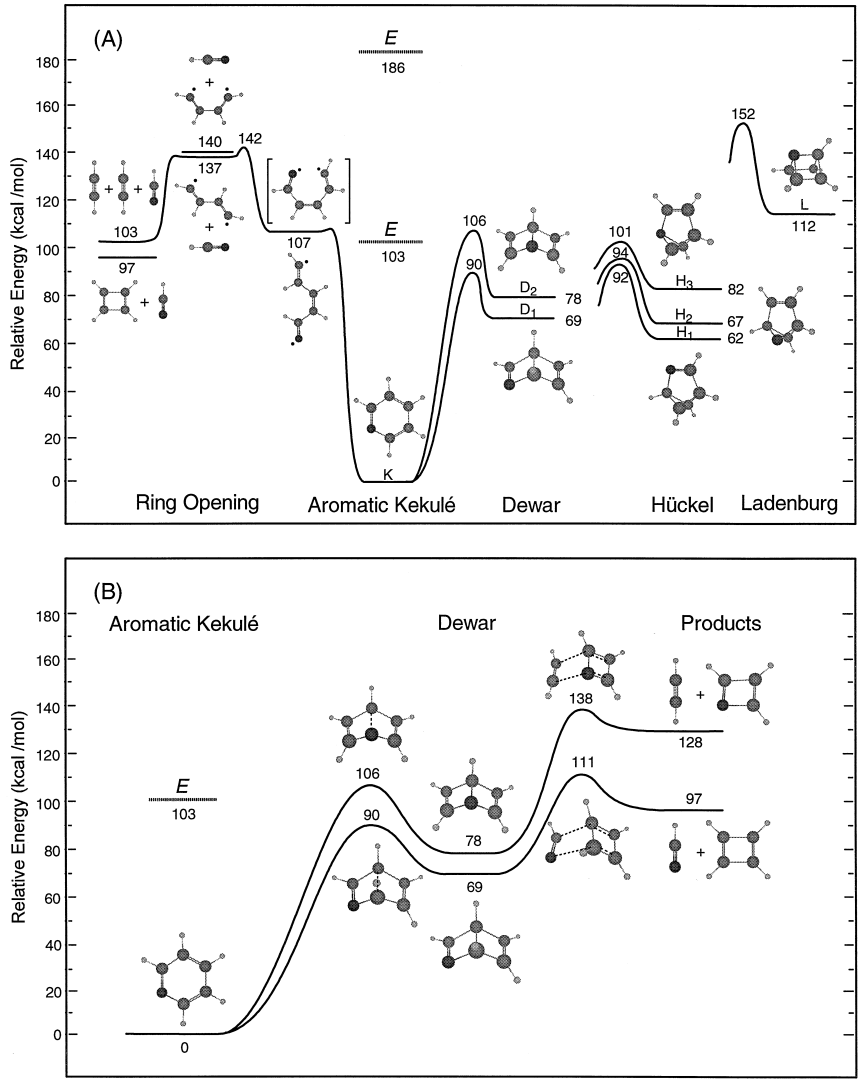

Fig. 2. Ground-state density functional theory/ab initio calculations. (A) The energetics and abbreviations of several possible valence-bond pyridine isomers as indicated. The related energy barriers have also been displayed. The values shown here are the G2M energies except those for the ring-opening channel which were obtained at the UB3LYP/6-311G(d, p) level. The energy of the ring-opening 'gauche' structure (non-optimized geometry shown in brackets) is close to that of the trans structure. Two excitation energies (E) are indicated by thick dashed lines. The transition state structures for some species are shown in Scheme 1. For discussion of other products and fulvene, see text for details. (B) Two different reaction pathways for the Kekulé structure to form two Dewar isomers through the bending motion. The dissociative process for both reactions involves a higher energy barrier, see text.

and to the Dewar. The structure of the transition state for the isomerization to the Hückel is similar to that which has been called prefulvene [9,10], but we have found that the TS in the lowest-energy path involves a twisted (five-atom nonplanar) geometry. The Hückel (benzvalene type) can also form tetrahedron C_4H_4 and HCN but this decomposition will involve a high energy barrier [11].

Similar DFT calculations were carried out for 2,6- and 3,5-dimethylpyridines at the B3LYP/6-31G(d)

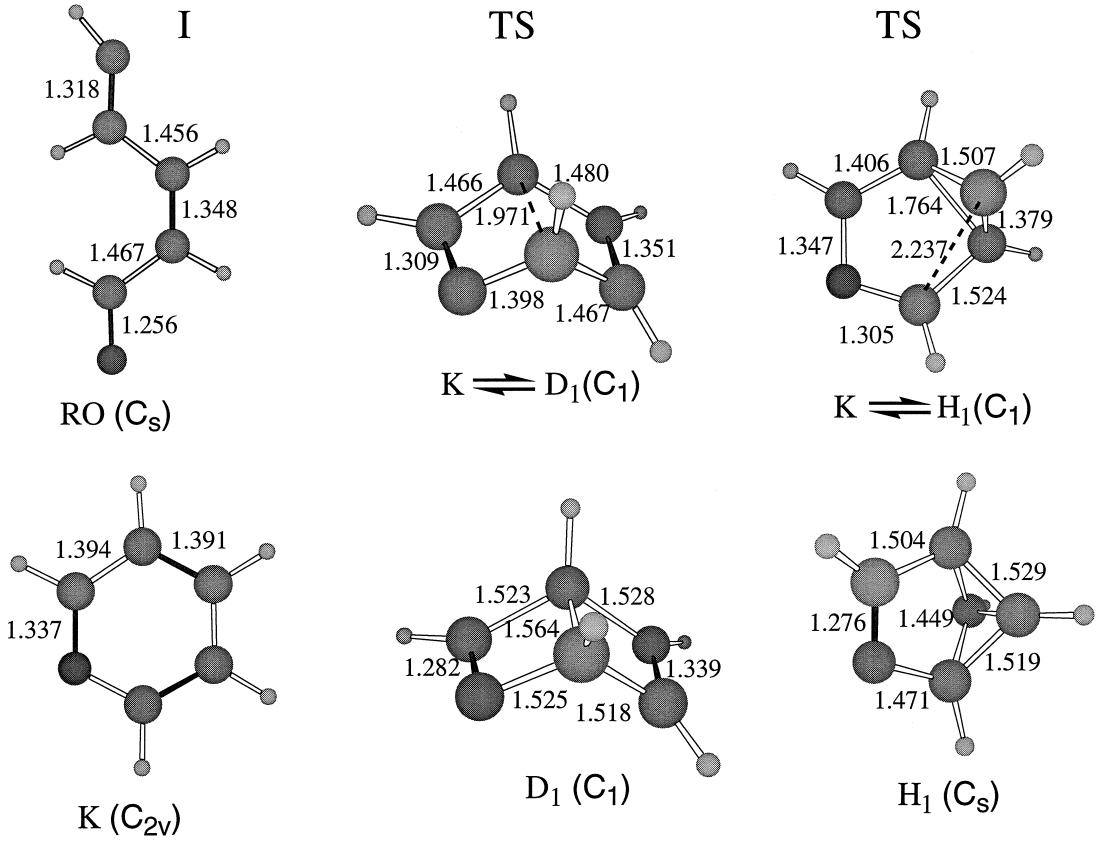

Scheme 1. Structures of transition states (TS), intermediate (I) and isomers obtained from our DFT calculations for some of the reaction paths of Fig. 2. K stands for aromatic Kekulé; D for Dewar; H for Hückel; and RO for ring opening. Double bonds are indicated by solid lines.

level. For pyridine-d_5, only the calculated zero-point energy was different from pyridine. We also made calculations for pyrimidine. For the ring-opening reaction of pyridine, the PES was calculated at the spin-unrestricted B3LYP/6-311G(d, p) level of theory because of the formation of an open-shell species, the ring-opened diradical intermediate [12]. All electronic structure calculations reported here were performed using G94 and G98 (Gaussian) packages.

4. Results and discussion

The mass spectrum and transients are shown in Figs. 3 and 4. The mass spectrum for pyridine (Fig. 3) only shows two peaks: the dominant parent (79 amu) and the C_4H_4 (52 amu). Transients were obtained for the individual mass peaks. For 277 nm excitation, the results are striking and exhibit both fs and ps dynamical processes. The C_4H_4 ion signal shows the same transient (not shown) as the parent, indicating its origin from the parent ion fragmentation. When the wavelength was changed to 282 nm, we observed similar behavior to the 277 nm case. For 288 nm excitation, i.e., below the S_1 transition, the transient signal disappears, indicating the one-photon nature of the excitation to the well-known $^1n\pi^*$ transition (see, e.g., Refs. [13,14]). This is confirmed by the lack of change of the general transient shape for pyridine when the pump energy ($< 5\ \mu J$) was attenuated by a factor of 2–3.

The total available energy in our experiment is 103 kcal/mol. Accordingly, only the isomerization

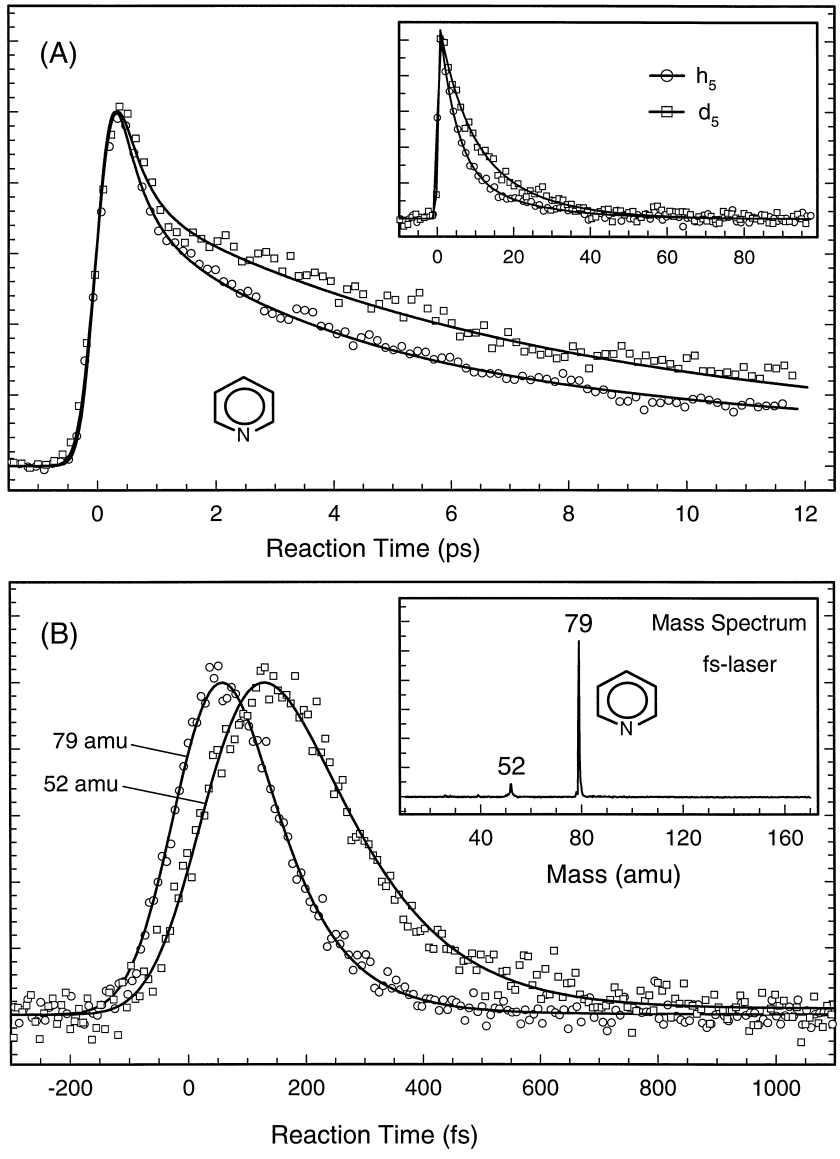

Fig. 3. (A) Transients of pyridine-h_5 and -d_5 (277 nm excitation) at short- and long-time ranges. A 10–20% non-decaying component (not shown) was present in the transients. (B) Mass spectrum of pyridine with fs laser ionization. The mass spectra are similar for both 277 nm and two-photon 307 nm excitation, and the parent signal is dominant. Transients (307/2 nm excitation) are shown for the 79 and 52 masses. Note the difference in time scale between (A) and (B).

pathways are possible (see Fig. 2). The transients exhibit a fast decay component of 400 fs and slower ones of 3.5 and 15 ps. All of the pyridine derivatives and deuteropyridine studied exhibit similar behavior, but the time constants increase (see Figs. 3 and 4). As discussed in Section 4.3, the non-aromatic structures are formed through the CI in less than 400 fs, and the time scales observed here are much shorter than the known spectroscopic lifetimes. In what follows, we discuss three major features of this work.

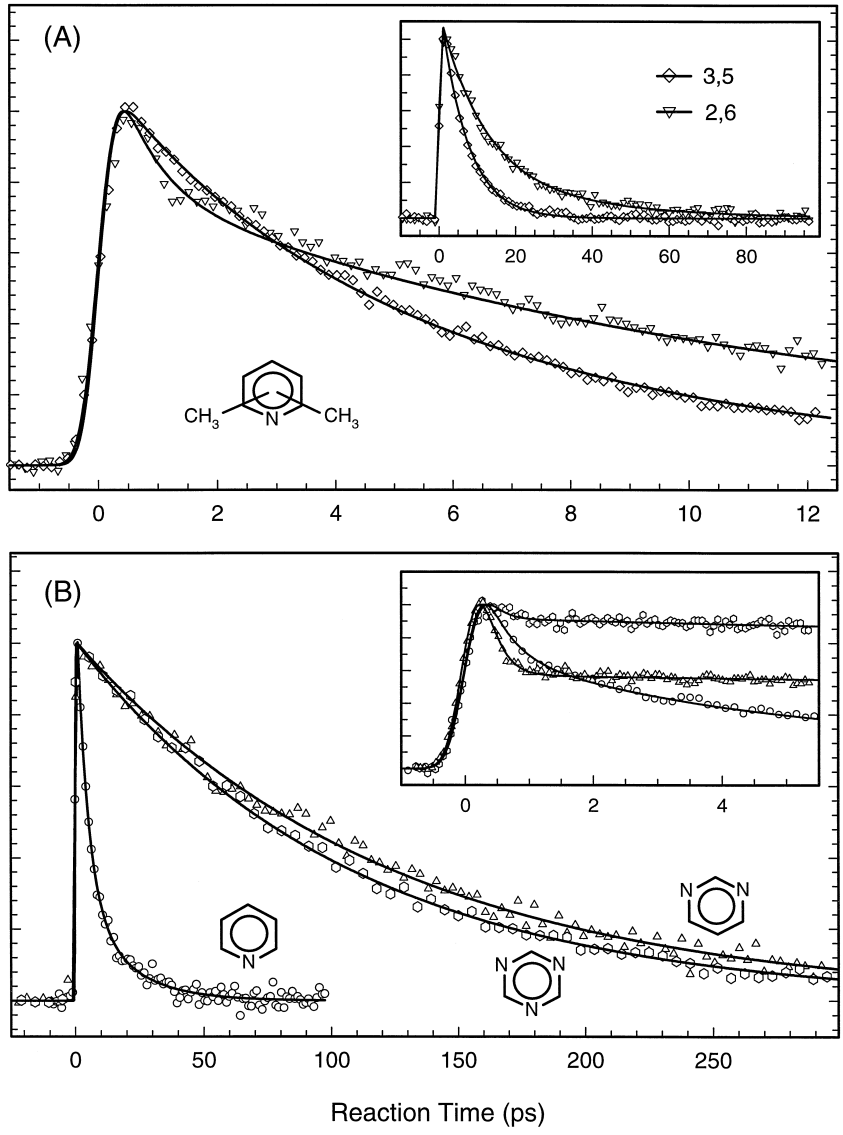

Fig. 4. (A) Transients obtained for 2,6- and 3,5-lutidine on short- and long-time scales. A 10–20% non-decaying component (not shown) was present in the transients. (B) Comparison of transients for different nitrogen substitution, pyridine, pyrimidine and triazine on the long- and short-time scales.

4.1. Dynamics of Dewar, Hückel and other structures

Among all isomers only D_1 and H structures allow for isomerization at our total energy of 103 kcal/mol (Fig. 2), and these are the isomers that give rise to the transient behavior. However, for all molecules studied, we observed a 10–25% non-decaying component on the ps time scale. This component reflects the contribution from the molecules on the upper surface that miss the CI region and stay in the local minima of the S_1 or T_1 state (Section 4.3).

The Dewar and Hückel isomers are structurally different from the aromatic Kekulé structure, but they have the same mass. On rearomatization, they isomerize to a highly vibrationally excited pyridine

and the effective ionization cross section becomes very small. The reverse process occurs on a much longer time scale in the μs to ms range because the barrier is high. Accordingly, the observed decay components of the parent signal in the ps range directly reflect the isomerization rates from the distinct Dewar- and Hückel-type structures to the excited aromatic Kekulé structure. Note that the Ladenburg structure can not be prepared at the available energies and neither is there enough energy to achieve any of the ring-opening processes (Fig. 2).

For pyridine-h_5, the transient in the ps range gives two apparent decay components, the 3.5 and 15 ps. From the DFT/ab initio calculations of the equilibrium energies and transition states, the faster decay is from the D_1 structure and the slower decay is from the H structures. Using our force field calculations, we obtained the total density and number of states and, thus, the statistical microcanonical rates. The RRKM calculations give the rates for the isomers in the ns range (1 ns for D_1, 29 ns for H_1, 17 ns for H_2, and 43 ns for H_3). The statistical RRKM rates differ from the experimental ones by three orders of magnitude. This is expected because, as discussed elsewhere [15], the CI is highly directional and on the fs time scale only selected vibrational modes are populated (non-statistical) [16]. However, it is interesting to note that the calculations indicate the two distinct time scales of D and H isomers and give the order of magnitude trend for the ratios.

For pyridine-d_5, the overall decay clearly becomes slower (Fig. 3A). For D_1 upon deuteration, the decay time of 3.5 ps increases to 5.1 ps, and for the H isomers the time is nearly the same, ~16 ps. The statistical calculations predict that both reaction times should lengthen by a factor of 3 (4) for D_1 (H_1), contrary to the observed almost doubling of the reaction time for D_1 and almost lack of change for H. This reflects difference in the motion of nuclei to form the transition states during the isomerization process. For the Dewar structure, all five deuterium atoms are involved in the bending motions at the transition state, but for the Hückel structure the C–C twisting is relatively localized and only two deuterium atoms participates effectively.

Methyl-group substitutions similarly lead to slower dynamics (Fig. 4A). From our DFT calculations, we find that methyl groups located on a double bond stabilize the isomer equilibrium structure. The D_1 isomers for 2,6- and 3,5-lutidine are stabilized by 3–4 kcal/mol, relative to pyridine. For both molecules, the isomerization barrier increases by 1–2 kcal/mol. Therefore, the reaction rates are expected to decrease, and the RRKM calculations give a reaction time in the 20–30 ns range as compared to 1 ns for the unsubstituted molecule. Experimentally, we obtained a reaction time of 10 ps for 2,6-lutidine and 6.5 ps for 3,5-lutidine, 3 to 2 times slower than pyridine. The reaction rate of 2,6-lutidine is slower than that of 3,5-lutidine because the barrier for the former is a little higher.

For the H_1 structure, the stabilization energy for 2,6- and 3,5-lutidine is ~1–2 kcal/mol. For 2,6-lutidine, the reaction barrier increases by ~1 kcal/mol, but it decreases by ~1 kcal/mol for 3,5-lutidine. The transition state for 3,5-lutidine is looser than that of 2,6-lutidine and has more low-frequency modes. The RRKM calculation predicts rate ratios of 80 times slower for 2,6-lutidine, but only 10 for 3,5-lutidine. Experimentally, we observed a ratio of $33/3.5 \approx 10$ for 2,6-lutidine, in the correct direction. For 3,5-lutidine, the long-decay component is not present, consistent with the predicted decrease of the ratio from 80 to 10 which will give time on the order of 6 ps. The reaction rates of 3,5-lutidine for both D and H structures are nearly the same, even though the Hückel isomer is more stable by ~5.5 kcal/mol and has a higher reaction barrier by ~6.5 kcal/mol. This can be ascribed to the loose nature of the transition state.

The general picture seen from the studies of pyridine was extended to other azines. For pyrimidine and triazine, the measured times are 113 and 106 ps, respectively. The fs decay component is actually faster than pyridine, 200 fs (Fig. 4B). Our DFT calculations show that the isomers of pyrimidine have similar energies and barriers as those of pyridine. Because of the observation of the early fs dynamics of the wave packet, the long ps components arise from the isomerization, similar to that of pyridine. However, because in the case of pyrimidine, the time is 30-fold longer than pyridine we must also include the spectroscopic lifetimes, which are ~100 ps at our energies [17]. For triazine, the reported results (277 nm or longer) suggest no or little direct fragmentation into HCN, and this system

is under further examination to compare with recent photodissociation studies of translational energy distributions by the Huber group [18].

4.2. The ring opening and fulvene channels

At the energy of 186 kcal/mol, the dynamics are drastically different. As noted in the mass spectrum, only the parent mass of pyridine and mass 52 were observed. The products of C_4H_4 (52) and HCN (27) are consistent with the reaction path shown in Fig. 2A. At the available energy of 193 nm (148 kcal/mol), the Lee group [11,19] observed several additional fragmentation channels, with the HCN plus C_4H_4 (believed to be 1,3-cyclobutadiene) being the major one.

The transient of mass 79 decays in 80 fs while that of mass 52 builds up in 80 fs and then disappears in 130 fs (Fig. 3B). Because the one-photon energy is below the S_1 transition, the results are from the two-photon excitation. The power dependence of the pump shows a close to quadratic behavior. The difference of the transients observed at 79 and 52 amu indicates that the signal at 52 amu is not due to ion fragmentation. The signal describes the dynamics of ring opening. The comparable times of the parent decay and the diradical fragment rise reveal that the fragment formation is directly related to the disappearance of the parent.

According to the DFT calculations in Section 3, ring opening of pyridine requires $\sim$ 110 kcal/mol to overcome the resonance energy and to break one C–N bond. This diradical (mass 79), originally in the 'gauche' configuration, actually is near the energy of the trans geometry (Fig. 2A). To eliminate HCN and form the cis or trans butadienyl diradical (mass 52), the molecule requires another $\sim$ 30 kcal/mol, breaking one C–C bond and forming a triple C–N bond. Thus, this transient species is formed in $\sim$ 80 fs and then evolves in 130 fs to form the final products (Fig. 2A): two acetylenes by C–C bond breakage; 1,3-cyclobutadiene by C–C bond closure; vinylacetylene by one hydrogen migration; and/or butatriene by a two-hydrogen migration.

It should be noted that there are three fulvene-type isomers and the most stable structure has an energy of 23.5 kcal/mol, predicted at the G2M level of theory. However, in order to form a fulvene-type isomer from the aromatic Kekulé and Hückel structures, the molecule needs to cross over a high energy barrier and this process involves the carbene (or nitrene) and/or prefulvene type of intermediates. Those intermediates lie at an energy of 102–112 kcal/mol based on the unrestricted DFT predictions.

4.3. Wavepacket motion: into the conical intersection

Following the fs laser preparation (Fig. 1), the packet, whose vibrational composition depends on the total energy, proceeds with two different types of *trajectories*; the reactive ones which go through the intersection region ('funnel') and the unreactive which are trapped in the 'spectroscopic' well. Accordingly, within the bending vibrational motion ($1/\nu \approx 80$ fs), the valence structure is distorted and vibrationally hot isomers are formed. However, the initial energy is deposited in the optically-allowed modes and energy must redistribute to other modes for the molecule to reach the intersection. This intramolecular vibrational energy distribution (IVR) process takes hundreds of fs. The nuclear bending and twisting motions are critical in making the 'forbidden' isomers. As the molecule bends or twists in the ground state, the energy rises because the motion is accompanied by strain and loss of the resonance energy – then new bond formation contributes to the total energy (see above). Concurrently, the upper surface lowers its energy (directly or through a barrier) as the molecule distorts its original structure, resulting in CI(s) [15,9].

The observed 200–700 fs component in all systems reported here reflects the initial displacement of the wavepacket and IVR in the reactive channel. For pyridine-h_5 and -d_5, this takes $\sim$ 400 fs. The decay time is not significantly different for both molecules because the bending and twisting motions, not the C–H motions, are mainly involved in the transformation; the excess energy in S_1 is $\sim$ 1260 cm^{-1} (3.6 kcal/mol), much lower than the C–H(D) frequency. For the 2,6-, 3,5-dimethyl, the process slows down to $\sim$ 650 fs (Fig. 4A). This is consistent with the fact that, on methylation, a blue-shift takes place [20] and the available vibrational energy decreases. Also, the total number of vibrational degrees of freedom increases. On the other hand, for pyrimidine and *s*-triazine, the process becomes faster, $\sim$ 200 fs (Fig. 4B), and this is because the S_1 state is red-shifted,

relative to pyridine, and the molecule (even with less vibrational modes) has more excess energy.

Evidence for the 'bifurcation' of the wave packet motion comes from the following observations:

(1) Our observed decay times in pyridine are much shorter than all reported times of fluorescence and internal conversion; 0.4–15 ps as opposed to 30–60 ps [17]. As shown by Yoshihara's group [17], the rates display an abrupt change with (small) excess vibrational energy; they suggest the importance of the isomerization channel of benzvalene form.

(2) The effect of methyl substitution on the observed rates is contrary to that observed for fluorescence in azines. As shown by Lim and co-workers [21], the proximity of the $n\pi^*$ to the $\pi\pi^*$ state leads to an enhanced internal conversion. Upon methylation, this conversion increases (not decreases) because of the decreased $n\pi^*-\pi\pi^*$ energy gap (~ 1800 cm^{-1} for 2,6-lutidine as opposed to 3600 cm^{-1} for pyridine [20]) and hence an increased overlap of wave functions S_1/S_0. In pyrazine, e.g., the nonradiative rate increases considerably upon methylation [21].

(3) All molecules studied show an underlying absorption continuum and some sharp bands; even in supersonic beams such continua do exist as shown in the careful study by Villa et al. [22]. This indicates that the wave packet motion is recurring in certain vibrational coordinates [23], but ultrafast dynamics due to the reactive channel must be part of the description. Even in three-atom systems, bifurcation of the wave packet from the transition state to final products is a general phenomenon due to the initial momenta and energy content of the packet [24,7]. It is interesting to note that the continuum absorption is present in many azines (Fig. 5) and that, in fact, the larger the sharp-band component, the more the nonreactive trapping. Spectral congestion is not the dom-

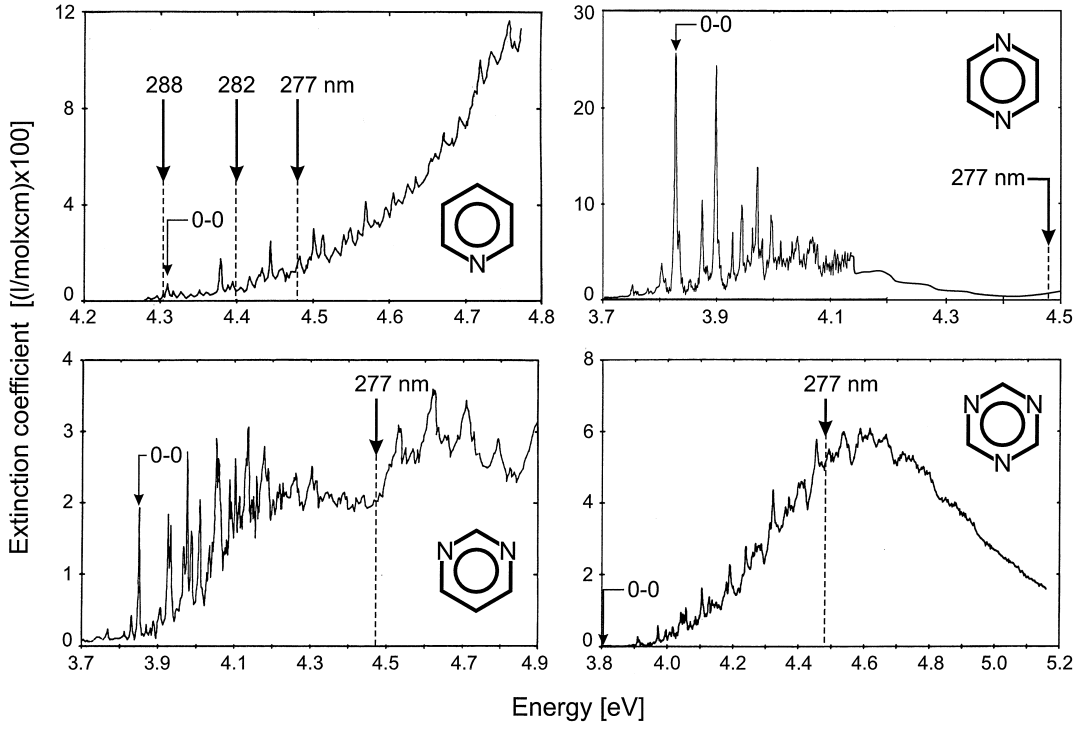

Fig. 5. Gas-phase absorption spectra of pyridine, pyrazine, pyrimidine and triazine (adapted form Ref. [13]). Indicated in the spectra are the $S_1 \leftarrow S_0$ (0–0) transitions and the experimental excitation wavelengths used in the present investigation. The two-photon 307 nm excitation of pyridine is not shown here. For pyrazine, the spectrum beyond 4.1 eV was reproduced, according to Ref. [13], and at 277 nm excitation the absorption is not enough to give strong transients although we did observe the mass spectra, primarily from the probe pulse (304 nm; 4 eV).

inant factor, especially at higher energies. Note that excitation spectra would not display features of the continuum and that nanosecond pulse excitation will bias the process to a much less continuum excitation.

(4) Our measurement of the transients with different polarizations did not result in a significant change in the time constants, consistent with our picture; the inertial decay should be several ps.

The above results are in agreement with product yield and species analysis [25,26]. They are also entirely consistent with photochemical experiments from Michl's group [27] involving the excitation of Dewar naphthalene and the conversion to naphthalene.

In concluding this section, we emphasize that elucidating the time scales observed for the different processes studied is the key to understanding the mechanism. We believe that such reactive pathways are general and important to many nonradiative processes in polyatomics. Bend motions promote the vibronic coupling as reported by Ito's group [28], and the valence distortion is evident in the studies of the spectroscopy (see the discussion in Ref. [22] for earlier relevant work, and Ref. [29] for showing the quasiplanarity in S_1). As shown in Fig. 1, the degree of distortion is linked to the branching of trajectories; when the distortion reaches outside the bound region, the reactive trajectories through CI dominate. The cases studied here show that lack of chemical fragmentation may lead to erroneous conclusion about the absence of CI-induced nonradiative return to the ground state and that the yield of products [30,31] has to be examined carefully. As such, our findings are relevant to the mysterious channel-3 process of benzene (see Refs. [9,10,32]). The fs initial reaction preparation is a key to observing the ultrafast nonadiabatic processes through the CI [15,33]. Work is in progress to study the possibility of other reactive isomers, the effect of vibrational heating and solvation in azines and benzenes.

Acknowledgements

This work was supported by the Office of Naval Research and by the National Science Foundation. TMB, a Feodor Lynen Fellow from the Alexander von Humboldt Foundation, acknowledges the foundation and Caltech for support. SDF, a postdoctoral fellow of the Fund for Scientific Research – Flanders, acknowledges a Fulbright scholarship and financial support by the Katholieke Universiteit Leuven and by Caltech. We thank Professor E.C. Lim for helpful discussion and Professor J. Michl for valuable insights and wonderful books.

References

[1] M. Klessinger, J. Michl, Excited States and Photochemistry of Organic Molecules, VCH, New York, 1995 (and references therein).
[2] F. Bernardi, M. Olivucci, M.A. Robb, Pure Appl. Chem. 67 (1995) 17.
[3] W. Domcke, G. Stock, Adv. Chem. Phys. 100 (1997) 1.
[4] D.R. Yarkony, Acc. Chem. Res. 31 (1998) 511.
[5] Y. Kobayashi, I. Kumadaki, Top. Curr. Chem. 123 (1984) 103.
[6] A.H. Zewail, Femtochemistry – Ultrafast Dynamics of the Chemical Bond, World Scientific, Singapore, 1994 (and references therein).
[7] D. Zhong, A.H. Zewail, J. Phys. Chem. A 102 (1998) 4031, and references therein.
[8] A.M. Mebel, K. Morokuma, M.C. Lin, J. Chem. Phys. 103 (1995) 7414.
[9] A.L. Sobolewski, W. Domcke, Chem. Phys. Lett. 180 (1991) 381.
[10] B.R. Smith, M.J. Bearpark, M.A. Robb, F. Bernardi, M. Olivucci, Chem. Phys. Lett. 242 (1995) 27.
[11] K.A. Prather, Y.T. Lee, Isr. J. Chem. 34 (1994) 43.
[12] A.A. Scala, E.W.-G. Diau, Z.H. Kim, A.H. Zewail, J. Chem. Phys. 108 (1998) 7933.
[13] A. Bolovinos, P. Tsekeris, J. Philis, E. Pantos, G. Andritsopoulos, J. Mol. Spectrosc. 103 (1984) 240.
[14] I.S. Walker, M.H. Palmer, A. Hopkirk, Chem. Phys. 141 (1989) 365.
[15] E.W.-G. Diau, O.K. Abou-Zied, A.A. Scala, A.H. Zewail, J. Am. Chem. Soc. 120 (1998) 3245.
[16] E.W.-G. Diau, J.L. Herek, Z.H. Kim, A.H. Zewail, Science 279 (1998) 847.
[17] I. Yamazaki, T. Murao, T. Yamanaka, K. Yoshihara, Faraday Discuss. Chem. Soc. 75 (1983) 395.
[18] T. Gejo, J.A. Harrison, J.R. Huber, J. Phys. Chem. 100 (1996) 13941.
[19] J.D. Chesko, Y.T. Lee, in: A.S. Mullin, G. Schatz (Eds.), Highly Excited Molecules, Am. Chem. Soc., Washington, DC, 1997, p. 107.
[20] I. Yamazaki, K. Sushida, H. Baba, J. Chem. Phys. 71 (1979) 381.
[21] E.C. Lim, Adv. Photochem. 23 (1997) 165, and references therein.
[22] E. Villa, A. Amirav, E.C. Lim, J. Phys. Chem. 92 (1988) 5393.

[23] R. Schinke, Photodissociation Dynamics, Cambridge University Press, New York, 1993.
[24] K. Möller, A.H. Zewail, Chem. Phys. Lett. 296 (1998) 619.
[25] O.L. Chapman, C.L. McIntosh, J. Pacansky, J. Am. Chem. Soc. 95 (1973) 614.
[26] D.E. Johnstone, J.R. Sodeau, J. Phys. Chem. 95 (1991) 165.
[27] S.L. Wallace, J. Michl, in: A.H. Zewail (Ed.), Photochemistry and Photobiology, vol. 2, Harwood, Chur, 1983, p. 1191.
[28] Y. Mochizuki, K. Kaya, M. Ito, J. Chem. Phys. 65 (1976) 4163.
[29] J.P. Jesson, H.W. Kroto, D.A. Ramsay, J. Chem. Phys. 56 (1972) 6257.
[30] K.E. Wilzbach, D.J. Rausch, J. Am. Chem. Soc. 92 (1970) 2178.
[31] E. Ratajczak, B. Sztuba, D. Price, J. Photochem. 13 (1980) 233.
[32] A.L. Sobolewski, C. Woywod, W. Domcke, J. Chem. Phys. 98 (1993) 5627.
[33] S.A. Trushin, W. Fuß, T. Schikarski, W.E. Schmid, K.L. Kompa, J. Chem. Phys. 106 (1997) 9386.